

Fig. 34—Photomicrographs illustrating features characteristic of internal rotation in an experimentally deformed dolomite single crystal. The internally rotated lamellae (L) are typically coarse and dark, and occasionally serrated. The rational lamellae (r) are straight, narrow, and sharply defined lines. X 175.

extended 12 per cent under 5-kb confining pressure, 24°C, at a constant strain rate of 1 per cent per minute. The specimen was extended normal to  $r_1$  (cleavage plane), an orientation favorable for basal ( $c\{0001\}$ ) translation. In thin section, the specimen is characterized by a central deformed sector bounded on either side by relatively undeformed sectors. The orientations of the  $c_v$  and cleavage are measured in the undeformed areas ( $c_v$  and  $r_1$ ) and in the deformed sector ( $c'_v$  and  $r'_1$ ). These are plotted in lower hemisphere equal-area projection (Fig. 35). It is apparent from their positions that there has been a clockwise external rotation of 12 degrees between the undeformed and deformed sectors. Detailed examination of the deformed sector reveals a coarse dark set of planar features ( $L_{r_1}^{c'}$ ) that make a small angle with  $r'_1$ . The normals to  $r'_1$  and  $L_{r_1}^{c'}$  lie on the same great circle as  $c'_v$ , which indicates that  $c'\{0001\}$  is the active gliding plane.\* Moreover, the

\*The active gliding plane and a rotated plane in all positions of rotation must be cozoal, i.e., share a common axis of intersection or rotation. Hence, the normals to these planes must lie on the same great circle.

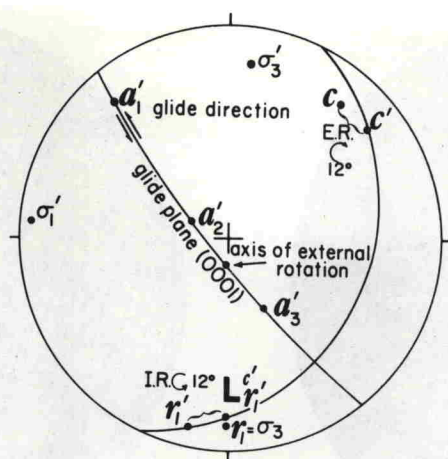


Fig. 35—Stereogram showing the internal and external rotation phenomena in experimentally deformed dolomite single crystal specimen No. 161 (from Higgs and Handin, Ref. 55). The specimen was extended 7.5 per cent under 5-kb confining pressure at 24°C. The least principal stress of the experiment ( $\sigma_3$ ) was oriented normal to  $r_1$  as indicated. External rotation of  $c$  to  $c'$  and  $r_1$  to  $r'_1$  and the internal rotation of  $r'_1$  to  $L^c_{r'_1}$  are shown.  $\sigma_1$  and  $\sigma_3$  are the stresses derived from translation gliding on  $c'$  along the  $a'_1$  gliding direction in the sense indicated. The angle between  $\sigma_3$  and  $\sigma'_3$  is 31 degrees.

angle between  $r'_1$  and  $L^c_{r'_1}$  indicates that a counterclockwise internal rotation of 12 degrees has occurred. Although  $c'$  is established as the active gliding plane, dynamic inferences still require identification of the direction and sense of shear. Basal translation can occur along any one of the three crystallographic  $a$  axes in either sense. As a first step, draw the great circle representing  $c'$ , i.e., the great circle normal to  $c'_v$  (Fig. 35). Because the rational position of  $r'_1$  is known, we can locate  $a'_1$ ,  $a'_2$ , and  $a'_3$  along the active gliding plane. One of these must be the gliding direction. This direction can be established from the axis of external rotation which must lie in the gliding plane and perpendicular to the gliding direction. Accordingly, the normal to the great circle through  $c_v$  and  $c'_v$  and to that through  $r_1$  and  $r'_1$  defines the axis of external rotation. Since this lies on the active gliding plane midway between  $a'_2$  and  $a'_3$ ,  $a'_1$  at 90 degrees to the axis of external rotation must be the gliding direction. Finally, the sense of shear is fixed by the sense of internal rotation. To bring  $r'_1$  to  $L^c_{r'_1}$  requires a left-lateral sense of shear along  $c'$  (Fig. 35).